ACKNOWLEDGMENTS AND ADDRESSES

Received June 4, 1969, from the *College of Pharmacy, University of Michigan, Ann Arbor, MI 48104*

Accepted for publication September 10, 1969.

Presented in part to the Basic Pharmaceutics Section, APhA Academy of Pharmaceutical Sciences, Miami meeting, May 1968.

Supported by Contract PH 43-68-1284 with Chemotherapy, National Cancer Institute, National Institutes of Health.

The authors thank the reviewer for suggesting Table II.

Rate of Crystal Growth of Sulfathiazole and Methylprednisolone

S. C. MEHTA, P. D. BERNARDO*, W. I. HIGUCHI, and A. P. SIMONELLI

Abstract □ The results of crystal growth rate studies using single crystals of sulfathiazole and methylprednisolone are presented. The growth rate of sulfathiazole crystals growing in a supersaturated aqueous solution showed stirring rate dependence from 10 to 400 r.p.m. The same stirring rate dependence was found for all three faces studied. In alcohol solutions, however, the stirring rate dependence appeared to disappear above 150 r.p.m., suggesting that at the higher stirring rates the rate of crystal growth of sulfathiazole is surface controlled. A plot of the growth rate *versus* the supersaturation ratio appeared to be linear for all studies with intercepts exhibited on the supersaturation ratio axis. The intercept appeared to be a function of its solvent varying from 1.07 to 1.43 and to be a function of the polarity of the alcohol. The crystal growth rate of methylprednisolone, on the other hand, showed no stirring rate dependence in the range from 20 to 400 r.p.m. and appears to be surface controlled even at low stirring rates.

Keyphrases □ Crystal growth rates—single crystal method □ Sulfathiazole crystals—growth rate □ Methylprednisolone crystals—growth rate □ Stirring rate effect—crystal growth □ Refractive index—crystal axes determination

There are a number of situations where an understanding of the growth behavior of crystals may provide a basis for improving pharmaceutical formulations. Crystal growth in a suspension formulation, as a result of temperature fluctuations or Ostwald ripening, may lead to undesirable changes in its particle-size distribution. Such changes whether they affect the ease of administration, efficacy, or the esthetic appearance of suspensions constitute "physical instability." Investigations (1–5) of crystal growth behavior involving systems of pharmaceutical interest are relatively few. Furthermore, most of these studies have not been mechanistically oriented, *i.e.*, aimed at establishing the molecular mechanisms. Generally such studies have only answered the question of whether or not crystal growth occurs under the particular prevailing condition.

The present report describes the results of crystal growth studies involving the two drugs, sulfathiazole and methylprednisolone. A simple but convenient method to study crystal growth is described. The crystal growth rate data were obtained as a function of supersaturation, crystal orientation, and stirring rate and provided much insight as to the probable rate-determining processes governing crystal growth. Furthermore, this method is well suited for the screening and evaluation of potential crystal growth inhibitors.

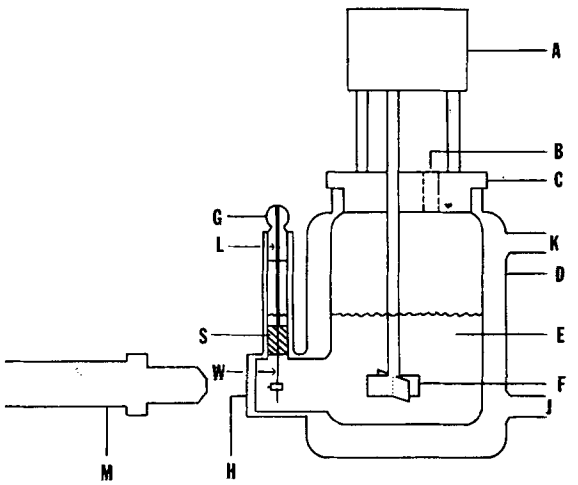

Figure 1—*Crystal growth apparatus. Key: A, synchronous motor; B, sampling port; C, Teflon lid; D, jacketed beaker; E, supersaturated solution; F, stirrer; G, glass stopper with a fused stainless steel rod (L); H, optical glass window; J, inlet for water (30°); K, outlet for water (30°); M, microscope; S, stainless steel coupling to hold removable crystal holder shown in Fig. 2; and W, tungsten wire holding crystal holder described in Fig. 2.*

GENERAL CONSIDERATIONS

Previous experiences have indicated the need to develop a technique utilizing a relatively convenient experimental system yet capable of providing much insight into the factors governing the rates of growth of crystals. Since the prime purposes of this study were the quantitation of crystal growth rates and the determination of the effect of various factors upon this growth, it was decided that a single crystal technique which measures linear growth rather than techniques which utilize gross volume changes should be employed. The single crystal technique is more reproducible and therefore more quantitative because of the following reasons:

1. Surface area is not important, as linear growth is a function of the chemical potential of the solution relative to the solid surface which can be expressed in terms of unit area. Furthermore, the

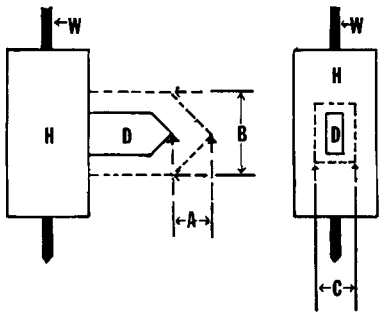

Figure 2—*Measurement of crystal growth. Key: H, inert rubber of crystal holder to keep crystal in position; D, original crystal; A, increase in half the length; B, increase in width; C, increase in thickness; and W, tungsten wire attached to stainless steel coupling (S) shown in Fig 1.*

same crystal can be exposed to a variety of conditions, all of which are affecting the same surface.

2. Nucleation does not present a problem as it is readily detectable. This is not true for the gross volume technique, and its presence must be determined by separate means such as a Coulter counter technique. If the proper growth rate is to be determined in a gross volume technique, the rate of nucleation must also be determined and its contribution subtracted.

3. The random heterogeneity of the surface free energy at the solid–liquid interface of all particles is not a problem in single crystal methods.

4. The need for a significant quantity of material to be transferred from the solution phase to the solid phase which causes the supersaturation ratio to be significantly decreased during experiments using the gross volume technique is also not present in single crystal work.

In addition, single crystal techniques, unlike gross volume techniques, not only permit the linear growth rate of each face of a crystal to be studied independently but also under varying conditions. This is essential in mechanistic studies. Finally the single crystal technique will also permit the crystal growth rate experiments to serve as a baseline for subsequent crystal growth inhibition studies. Furthermore, in order to separate diffusion-controlled cases from surface-controlled rates, it was decided to employ variable stirring conditions as well as varying supersaturation conditions.

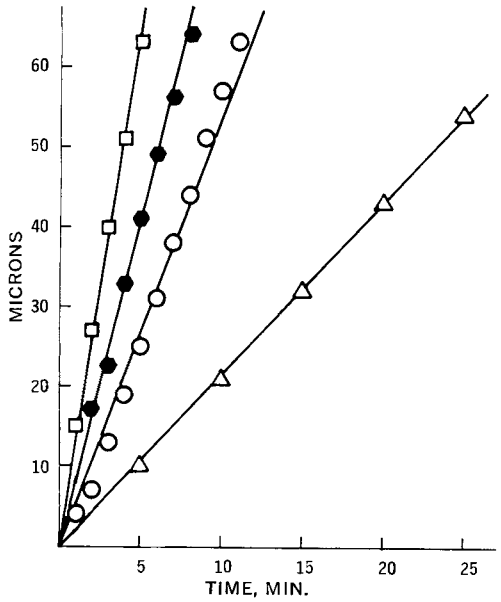

Figure 3—*Crystal growth of sulfathiazole in 95% v/v ethanol along the long axis at different supersaturation ratios. Key: △, S = 1.26; ○, S = 1.37; ●, S = 1.52; and □, S = 1.73.*

Table I—Solubility of Sulfathiazole and Methylprednisolone in Different Solvent Systems at 30°

Solvent	Solubility, g./100 g.	$\lambda_{max.}$, mμ
Sulfathiazole		
Water	0.065	282
95% v/v Ethanol in water	1.06	288
50% v/v Ethanol in water	1.30	
60% v/v Ethanol in *sec*-butanol	0.555	
Methylprednisolone		
Water	0.0072	249
1% v/v Ethanol in water	0.0077	
2% v/v Ethanol in water	0.0085	

MATERIALS

All solvents utilized in the experiments were distilled. The sulfathiazole crystals used in the crystal growth experiments were prepared by double recrystallization either from 95% ethanol or from water. The methylprednisolone crystals used in these studies

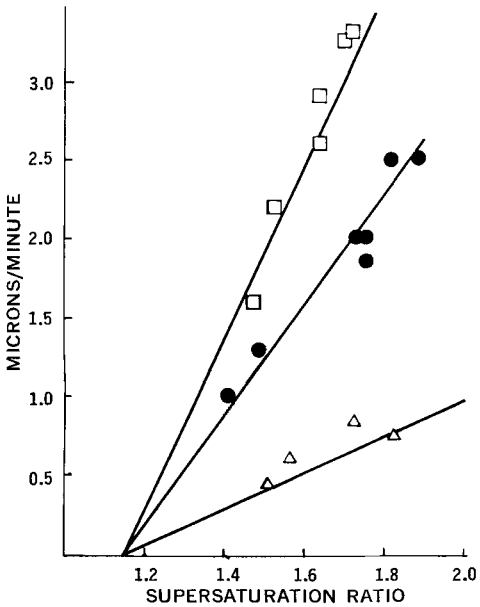

Figure 4—*Crystal growth rate of sulfathiazole in water along the long axis of the crystal as a function of supersaturation at different stirring speeds. Key: △, 10 r.p.m.; ●, 150 r.p.m.; and □, 400 r.p.m.*

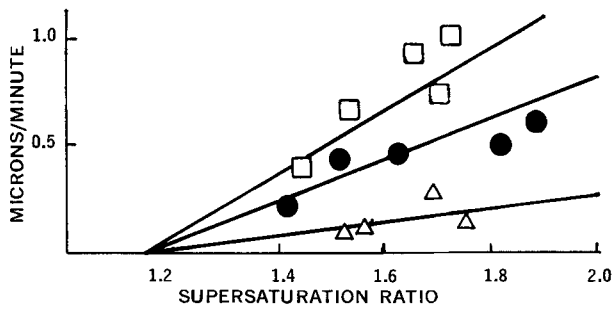

Figure 5—*Crystal growth rate of sulfathiazole in water along the dimension designated as width as a function of supersaturation at different stirring speeds. Key: △, 10 r.p.m.; ●, 150 r.p.m.; and □, 400 r.p.m.*

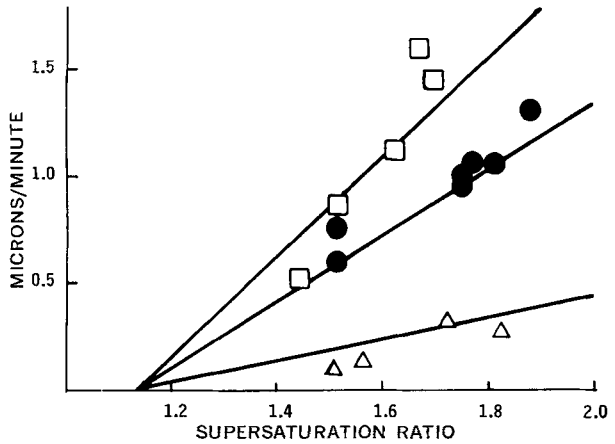

Figure 6—*Crystal growth rate of sulfathiazole in water along the dimension designated as thickness as a function of supersaturation at different stirring speeds. Key: △, 10 r.p.m.; ●, 150 r.p.m.; and □, 400 r.p.m.*

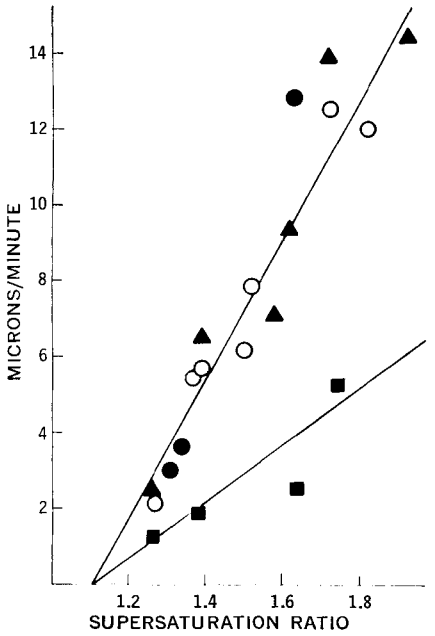

Figure 7—*Crystal growth rate of sulfathiazole in 95% v/v ethanol along the dimension designated as the long axis as a function of supersaturation at different stirring speeds. Key: ■, 10 r.p.m.; ○, 150 r.p.m.; ●, 240 r.p.m.; and ▲, 400 r.p.m.*

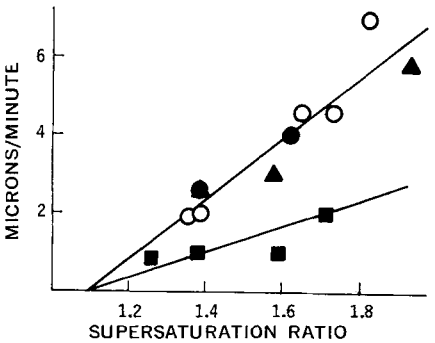

Figure 8—*Crystal growth rate of sulfathiazole in 95% v/v ethanol along the dimension designated as width as a function of supersaturation at different stirring speeds. Key: ■, 10 r.p.m.; ○, 150 r.p.m.; ●, 240 r.p.m.; and ▲, 400 r.p.m.*

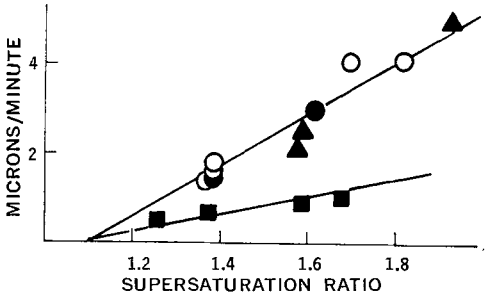

Figure 9—*Crystal growth rate of sulfathiazole in 95% v/v ethanol along the dimension designated as thickness as a function o supersaturation at different stirring speeds. Key: ■, 10 r.p.m.; ○, 150 r.p.m.; ●, 240 r.p.m.; and ▲, 400 r.p.m.*

were prepared by recrystallization either from a 50% v/v alcohol–water mixture or from acetone.

The crystalline modifications of both compounds were the same as those designated as the most stable forms (Form I) in previous studies (6, 7) and were confirmed by melting point, refractive index, X-ray diffraction, and IR spectra.

In addition, refractive index determinations were used to characterize the long axes of the individual crystals of both compounds. The refractive index of the long axis of the hexagonally shaped face of sulfathiazole crystal was found to be 1.674, in agreement with the reported value (8). For methylprednisolone the refractive index along the long axis of the rod-shaped crystal was found to be 1.602 (9).

The supersaturated solutions used in these studies were prepared by either of two methods, saturating at higher temperatures using steam heat or by solvent mixing. Because of chemical instability, supersaturated methylprednisolone solutions were always prepared by solvent mixing.

APPARATUS AND PROCEDURE

Figure 1 shows the apparatus used to study the growth rate of sulfathiazole. The temperature of the system was controlled at 30°

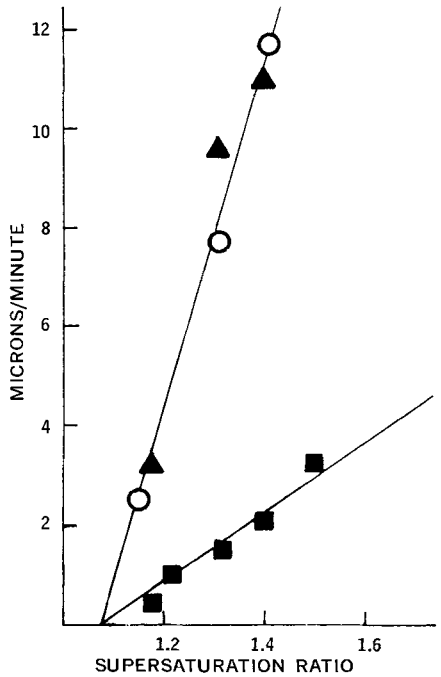

Figure 10—*Crystal growth rate of sulfathiazole in 50% v/v ethanol–water along the long axis as a function of supersaturation at different stirring speeds. Key: ■, 10 r.p.m.; ○, 150 r.p.m.; and ▲, 400 r.p.m.*

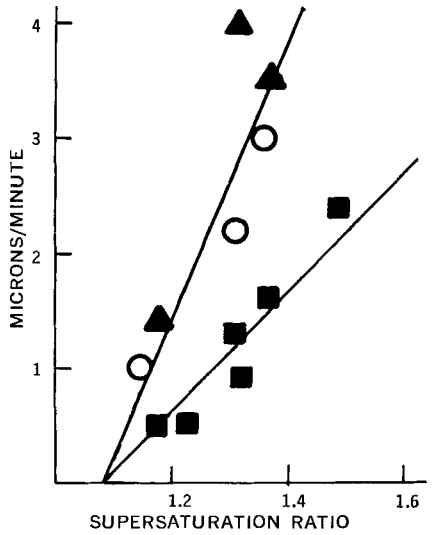

Figure 11—*Crystal growth rate of sulfathiazole in 50% v/v ethanol–water along the dimension designated as width as a function of supersaturation at different stirring speeds. Key: ■, 10 r.p.m.; ○, 150 r.p.m.; and ▲, 400 r.p.m.*

by means of a water jacket through which 30° water was circulated. For crystal growth studies, a single crystal of sulfathiazole is mounted in a slit made in a piece of rubber for this purpose (10). See Fig. 2. This piece of rubber is held by a tungsten wire attached to a stainless steel coupling. This coupling permits the crystal holder to be removed to facilitate the delicate and tedious process of mounting the crystal. In addition the coupling prevents the crystal from lateral movement during the experiment after the crystal holder is mounted in place. After a mounted crystal is immersed in the supersaturated solution, a microscope calibrated in microns is used to study crystal growth through an optical-glass window. Figure 2 shows the manner in which the length, width, and thickness of a crystal are followed as a functon of time. The supersaturated solution was stirred at a constant rate during an experiment by means of a synchronous motor mounted on the container lid. The effect of the stirring rate on crystal growth rate, on the other hand, was studied by interchanging motors of different speeds. A stopwatch was used to obtain the time of each crystal measurement. During the experiment, samples were periodically withdrawn from the solution and assayed spectrophotometrically in order to determine the concentration of the solution.

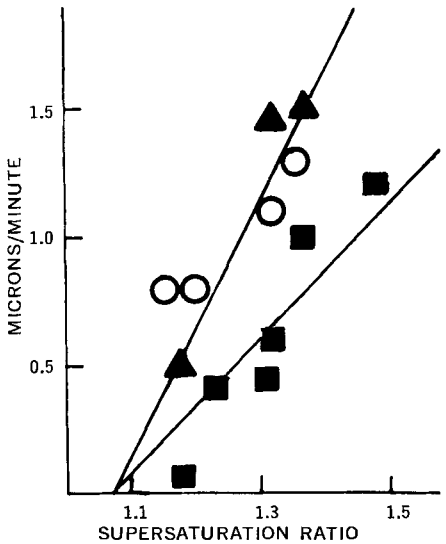

Figure 12—*Crystal growth rate of sulfathiazole in 50% v/v ethanol–water along the dimension designated as thickness as a function of supersaturation at different stirring speeds. Key: ■, 10 r.p.m.; ○, 150 r.p.m.; and ▲, 400 r.p.m.*

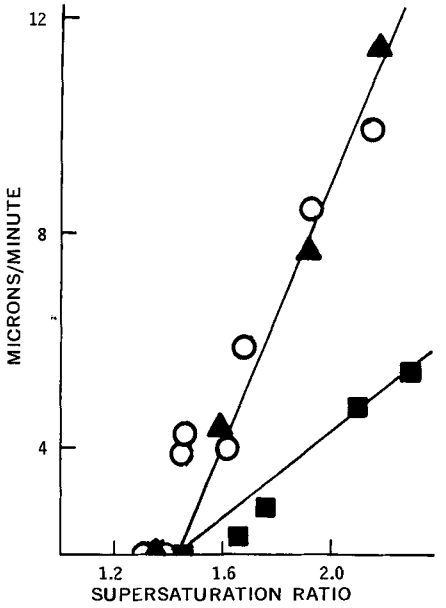

Figure 13—*Crystal growth rate of sulfathiazole in 40% v/v sec-butanol–60% v/v ethanol along the long axis as a function of supersaturation at different stirring speeds. Key: ■, 10 r.p.m.; ○, 150 r.p.m.; and ▲, 400 r.p.m.*

RESULTS AND DISCUSSION

The solubilities of sulfathiazole and methylprednisolone were determined in the following manner. Excesses of the amounts of the recrystallized compounds needed to produce saturated solutions

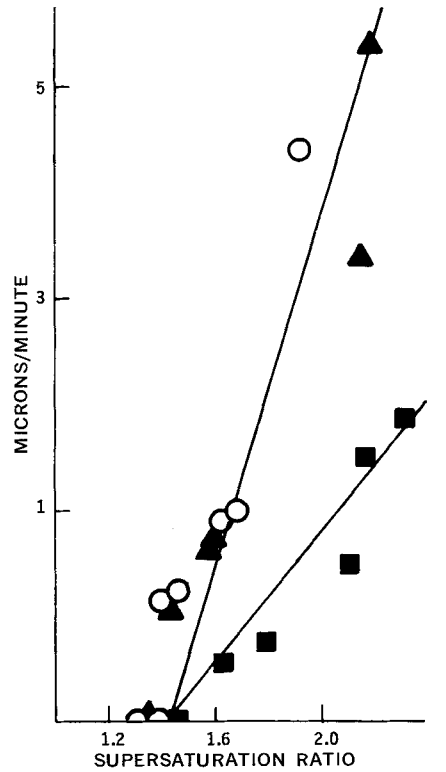

Figure 14—*Crystal growth rate of sulfathiazole in 40% v/v sec-butanol–60% v/v ethanol along the axis designated as width as a function of supersaturation at different stirring speeds. Key: ■, 10 r.p.m.; ○, 150 r.p.m.; and ▲, 400 r.p.m.*

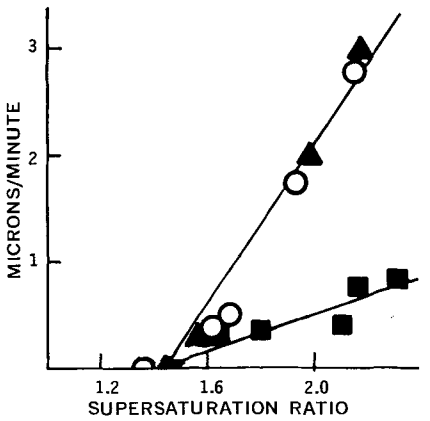

Figure 15—*Crystal growth rate of sulfathiazole in 40% v/v sec-butanol–60% v/v ethanol along the axis designated as thickness as a function of supersaturation at different stirring speeds. Key:* ■, *10 r.p.m.;* ○, *150 r.p.m.; and* ▲, *400 r.p.m.*

were placed in volumetric flasks with the solvents and agitated in a water bath at 30°. Duplicate samples were withdrawn at 12–24-hr. intervals, filtered through a 0.45-μ Millipore filter, and analyzed spectrophotometrically. The solubilities of sulfathiazole and of methylprednisolone in the various solvents used are listed in Table I.

Sulfathiazole Studies—Figure 3 represents the results of a typical sulfathiazole crystal growth experiment in 95% v/v ethanol where the growth in microns along the long axis was measured and plotted as a function of time. The growth–time plots were always found to be linear with little scatter, except in cases where the apex of the crystals was initially not sharp due to prior washing in a solvent. In the latter situations the slopes of the plots became linear after a short initial period during which time sharpening of the crystal edges occurred. Size variations of the crystals employed in these experiments were found to have little or no effect upon the rate of growth over a crystal length range of 450 to 2000 μ. Also the method of preparation of the seed crystals usually had no effect upon the growth rates.

From limiting linear portions of the data such as those presented in Fig. 3, the rates were obtained by determining the slopes for each experiment and are plotted in Figs. 4–15 for each of the three dimensions of the sulfathiazole crystal in a number of solvents under different stirring rates. These rates have been presented as a function of the supersaturation ratio, S, which is the supersaturated solution concentration divided by the solubility. The data for sulfathiazole crystal growth studies in water (Figs. 4–6) appeared to be linearly dependent upon the supersaturation ratio, S, for all stirring speeds and for all three dimensions. Least-squares parameters calculated for these studies are tabulated in Table II and showed that a common intercept of $S = 1.17$ was consistent with all of the water experiments.

The stirring rate dependence found in these experiments strongly supports a diffusion-controlled process in region $S > 1.17$.

Table II—Linear Least-Squares Parameters[a] for Sulfathiazole Using Water as a Solvent

Axis	Stirring, r.p.m.	Intercept[b]	Av. Intercept	Slope[c]
Length	10	0.99	1.10	1.26
	150	1.09		3.41
	400	1.22		5.56
Width	10	1.33	1.24	0.04
	150	1.08		1.67
	400	1.31		2.54
Thickness	10	1.27	1.16	0.29
	150	1.01		0.84
	400	1.20		1.59
Av. for all data		1.17		

[a] See *Appendix*. [b] Both slope and intercept were allowed to vary. [c] Curve was forced through average intercept for all three axes, $S = 1.17$.

Table III—Linear Least-Squares Parameters[a] for Sulfathiazole Using 95% Hydroalcoholic Solution as a Solvent

Axis	Stirring, r.p.m.	Intercept[b]	Av. Intercept	Slope[c]
Length	10	1.15	1.14	6.89
	150	1.10		18.00
	240	1.22		21.63
	400	1.09		18.46
	150, 240, 400	1.12		18.62
Width	10	0.94	1.05	2.95
	150	1.17		8.40
	400	1.04		7.20
	150, 400	1.11		7.91
Thickness	10	0.80	1.08	1.90
	150	1.16		5.90
	400	1.29		5.50
	150, 400	1.17		5.70
Av. for all data		1.10		

[a] See *Appendix*. [b] Both slope and intercept were allowed to vary. [c] Curve was forced through average intercept for all three axes, $S = 1.10$.

The growth rates of all of the dimensions appear to be determined by the transport of solute through the solvent at even the highest stirring speeds. For comparison purposes, the growth rate curves as a function of the stirring rate shown by Figs. 4, 5, and 6 were arbitrarily fitted by linear curves passing through the 1.17 intercept, with arbitrary slopes chosen so that a constant slope ratio as a function of the stirring rate was maintained in all three figures; *i.e.*, the ratios of the slope at 400 r.p.m. to that at 150 r.p.m. to that at 10 r.p.m. was constant. The agreement of these arbitrary curves with the experimental data points strongly suggests that the stirring rate dependence is the same for all three dimensions.

The intercept value of about $S = 1.17$ might be related to a "critical" supersaturation for two-dimensional nucleation. Therefore, at very low supersaturation ratios, crystal growth may occur extremely slowly or may be dependent upon the existence of screw dislocations.

Sulfathiazole crystal growth experiments with the other solvent systems studied (Figs. 7–15) generally appeared to show stirring rate dependence at the lower speeds but interestingly the rates were much less stirring dependent at the higher speeds in these solvents than in the water experiments. The growth rates observed in 95% v/v ethanol, 50% ethanol–water, and 40% butanol–60% ethanol were found to be essentially independent of stirring rates above 150 r.p.m. The growth rates at 10 r.p.m. were generally much slower in these studies See Tables III–V.

These experiments in the alcohol-containing solvents appear to be consistent with the interpretation that at lower agitation conditions (~10 r.p.m.) the crystal growth rates are solvent diffusion controlled at the higher supersaturations. However, at higher

Table IV—Linear Least-Squares Parameters[a] for Sulfathiazole Using 50% Hydroalcoholic Solution as a Solvent

Axis	Stirring, r.p.m.	Intercept[b]	Av. Intercept	Slope[c]
Length	10	1.13	1.10	6.97
	150	1.08		33.55
	400	1.08		34.78
	150, 400	1.08		34.17
Width	10	1.14	1.08	5.08
	150	1.04		9.98
	400	1.05		13.34
	150, 400	1.05		11.77
Thickness	10	1.15	1.02	2.70
	150	0.84		4.87
	400	1.08		5.27
	150, 400	0.98		5.07
Av. for all data		1.07		

[a] See *Appendix*. [b] Both slope and intercept were allowed to vary. [c] Curve was forced through average intercept for all three axes, $S = 1.07$.

Table V—Linear Least-Squares Parameters[a] for Sulfathiazole Using 40% *sec*-Butanol–60% Ethanol as a Solvent

Axis	Stirring, r.p.m.	Intercept[b]	Av. Intercept	Slope[c]
Length	10	1.53	1.39	6.27
	150	1.33		21.04
	400	1.30		15.39
	150, 400	1.29		13.13
Width	10	1.52	1.40	2.01
	150	1.27		5.91
	400	1.42		6.49
	150, 400	1.31		5.17
Thickness	10	1.41	1.50	0.90
	150	1.56		3.57
	400	1.52		3.86
	150, 400	1.54		4.67
Av. for all data		1.43		

[a] See *Appendix*. [b] Both slope and intercept were allowed to vary. [c] Curve was forced through average intercept for all three axes, $S = 1.43$.

stirring rates, the crystal growth rates are surface controlled rather than diffusion controlled.

In all the plots shown in Figs. 7–15, there appear to be significant intercepts on the supersaturation axes as were found to be the case in the water experiments Figs. 4–6. In the cases of ethanol and ethanol–water experiments, the intercepts are the order of $S \simeq 1.1$. For the 40% *sec*-butanol–60% ethanol the intercept is much larger, the order of $S \simeq 1.43$. These intercepts might again be related to the "critical" supersaturation for two-dimensional nucleation in the respective solvents. It is noteworthy to mention at this point that in *n*-propanol, crystal growth of sulfathiazole did not occur even at supersaturation of 2.2, and that in *sec*-butyl alcohol a supersaturation ratio of 5.5 showed no growth. The observations in conjunction with the *S*-intercepts found in the present studies suggest a direct relationship between the "critical *S*" for two-dimensional nucleation and alcohol solvent polarity—*viz.*, the higher the alcohol solvent polarity the smaller the *S*-intercept.

METHYLPREDNISOLONE CRYSTAL GROWTH IN WATER

The growth rate along the rod axis (refractive index = 1.602) of the methylprednisolone crystal in water at various supersaturations and stirring speeds was also studied. The results are shown in Fig. 16. The data at all stirring speeds appear to be linear with supersaturation and show a small intercept on the *S*-axis. The least-squares linear curves were calculated and the slopes and intercepts tabulated in Table VI. As opposed to sulfathiazole crystals, Table VI clearly shows that the rates for methylprednisolone appeared to be virtually independent of stirring for all stirring rates over the range of 20 to 400 r.p.m. This supports a mechanism in which the crystal growth rate of methylprednisolone in water is surface controlled in the range of agitation rates employed in these studies.

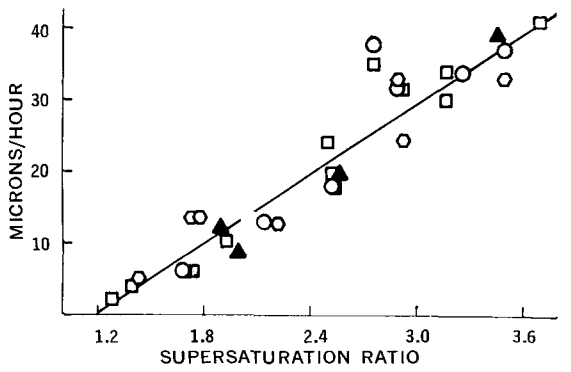

Figure 16—*Crystal growth rate of methylprednisolone in water as a function of supersaturation at different stirring speeds. Key:* ▲, *20 r.p.m.;* □, *150 r.p.m.;* ○, *240 r.p.m.; and* ⬡, *400 r.p.m.*

Table VI—Linear Least-Squares Parameters for Methylprednisolone Using Water as the Solvent

Stirring, r.p.m.	Intercept[a]	Slope[a]
20	1.43	18.732
150	1.27	17.498
240	1.37	19.163
400	0.90	13.329
All data points	1.23	16.896

[a] Both slope and intercept were allowed to vary.

For this reason a least-squares linear curve was calculated using all the methylprednisolone growth rates regardless of stirring rate, and this curve was drawn in Fig. 16.

SUMMARY

These results show the advantage of using a single crystal technique to obtain quantitative data regarding the growth rate of crystalline drugs. In particular, it permits meaningful quantitation of the stirring rate dependence and the effect of the composition of the solution on the crystal growth rate. This permits an insight as to the controlling mechanism operative under the conditions of the experiment.

APPENDIX: LEAST-SQUARES PARAMETERS

It is generally accepted that the results of a least-squares optimization of the data will depend on the function chosen, *i.e.*, straight line, parabola, exponential, *etc.* It is not always recognized, however, that one must be careful to use the appropriate least-squares treatment if one is to fit the best linear curve to the experimental data. For example, one can assume that the experimental error resides solely in the y data, in the x data, or in both. Obviously the best fit curve obtained will depend on which approach was used.

It also should be noted that the least-squares approach (a mathematical interpretation as opposed to a physical interpretation) should not contradict any known facts and/or limitations set by the experimental system. For example, if it is known that the data plot passes through the origin, then a least-squares set of equations which ignores this requirement may not only result in an artificial intercept but also an incorrect slope.

By definition, a crystal must be exposed to a supersaturation ratio greater than 1 in order for it to grow. Therefore, any optimization of the authors' data that yields a curve which displays a positive y-intercept must be incorrect. This means the least-squares approach to be used must yield an x-intercept of the supersaturation ratio axis if the most correct slope is to be calculated.

In addition, it is reasonable to assume that all curves of a given system should be represented by the same intercept for the following reason. At the x-intercept, the crystal growth is obviously independent of the stirring rate and most likely is regulated by a surface-controlled process. If this is true, all curves must intercept at the same point as the only difference between curves is the stirring rate.

With the above in mind, the following approach was arbitrarily used to determine the intercepts and slopes for the systems studied. First the least-squares parameters were determined allowing both the intercept and slope to vary, *i.e.*, $y = mx + b$ where m is the slope and the x-intercept is b/m. The average x-intercept for all curves in a given system was calculated and assumed to be the best estimate of the supersaturation ratio axis intercept. The best estimate for the slope of each curve was then determined using the least-squares equations for $y = m(x - \bar{I})$, where $\bar{I}$ is the average intercept for the system.

REFERENCES

(1) J. K. Dale and S. L. Ross, U. S. pat. 2,861,920, Nov. 25, 1958.

(2) J. K. Dale and R. A. Hanze, U. S. pat. 3,062,712, Nov. 6, 1962.

(3) J. Polderman, *Bull. Chim. Pharm.*, **101**, 105(1962).

(4) J. E. Carless and A. A. Foster, *J. Pharm. Pharmacol.*, **18**, 697(1966).
(5) J. Glasby and K. Ridgway, *ibid.*, **20**, 94S(1968).
(6) H. Nogami and T. Nagai, *Yakkyoku*, **9**, 29(1958).
(7) J. Hasegawa and T. Nagai, *Chem. Pharm. Bull. (Tokyo)*, **6**, 129(1958).
(8) D. C. Grove and G. L. Keenan, *J. Amer. Chem. Soc.*, **63**, 97(1941).
(9) J. A. Biles, *J. Pharm. Sci.*, **50**, 464(1961).
(10) D. J. Allen, G. Milosovich, and A. M. Mattocks, *ibid.*, **54**, 383(1965).

ACKNOWLEDGMENTS AND ADDRESSES

Received June 4, 1969, from the *College of Pharmacy, University of Michigan, Ann Arbor, MI 48104*

Accepted for publication November 20, 1969.

Presented in part to the Basic Pharmaceutics Section, APhA Academy of Pharmaceutical Sciences, Dallas meeting, April 1966.

* Present address: Smith Kline & French Laboratories, Philadelphia, Pa.

Theoretical Model Studies of Drug Absorption and Transport in the Gastrointestinal Tract I

AKIRA SUZUKI, W. I. HIGUCHI, and N. F. H. HO

Abstract □ The simultaneous chemical equilibria and mass transfer of basic and acidic drugs through a two-phase compartment model were theoretically investigated. The model consisted of a well-stirred bulk aqueous phase, an aqueous diffusion layer, and a lipid barrier for perfect and imperfect sink cases. The nonsteady and quasi-steady-state changes in the concentration–distance distributions in the lipid phase were studied. The rate of change of the total drug concentration in the bulk aqueous phase was described in the general form of a first-order equation useful for the evaluation of experiments. A limiting steady-state relationship involving the transport rate with the partition coefficient, pH at the aqueous–lipid interface, dissociation constant of the drug, aqueous and lipid diffusion coefficients, and thickness of the diffusion layer was derived. Increasing the agitation rate in the aqueous phase markedly affects the pH profiles for the rate of transport. The pH-partition theory is shown to be a limiting case of the more general approach presented.

Keyphrases □ Drug absorption, transport—theoretical model □ Model, two-phase compartment—theoretical investigation □ Chemical equilibria, mass transfer—two-phase compartment model □ Agitation rate effect—rate transport pH profiles

The increasing interest in the mechanistic understanding rather than in only a mathematical representation of drug transport and absorption phenomena should dictate systematic physical model analyses of various *in vitro* situations. Thus, detailed theoretical considerations of diffusion and equilibria involving multibarrier systems and the carrying out of appropriate model experiments are necessary for the isolation of the important *in vivo* factors.

Recent investigations (1–4) in these laboratories have been devoted to the physical model approach to a number of situations in this regard. The present paper is concerned with the problem of treating the time dependency and the pH-buffer dependency for the transport of basic and acidic solutes into and across lipoidal barriers. It is, to some extent, an extension of the works of Howard *et al.* (3) and Stehle (4) and should be useful in the understanding of gastrointestinal and buccal absorption problems. In the accompanying paper (5), the techniques developed here are applied to some of the data on *in situ* drug absorption published by Koizumi *et al.* (6, 7).

THEORY

General Description of the Model—The simultaneous mass transfer and chemical equilibrium reactions in a system consisting of two homogeneous phases will follow the one-dimensional model in Fig. 1. The bulk aqueous phase is well stirred and consists of a basic drug and buffer. At $x \leq -h$,

$$(TR)_{-h} = (R)_{-h} + (RH^+)_{-h} \quad \text{(Eq. 1)}$$

$$(TB)_{-h} = (B^-)_{-h} + (HB)_{-h} \quad \text{(Eq. 2)}$$

where (TR) is the total drug concentration of R and RH^+ species and (TB) is the total buffer concentration of B^- and HB species. It is assumed that electrical neutrality holds everywhere in the aqueous phase. Consequently, at $x \leq 0$,

$$(H^+) + (RH^+) + (Na^+) - (OH^-) - (B^-) = 0 \quad \text{(Eq. 3)}$$

where (Na^+) is the cation concentration derived from the buffer. It is further assumed that the following equilibrium reactions are instantaneous,

$$\frac{(R)(H^+)}{(RH^+)} = K_{a,R} \quad \text{(Eq. 4a)}$$

$$\frac{(B^-)(H^+)}{(HB)} = K_{a,HB} \quad \text{(Eq. 4b)}$$

$$(H^+)(OH^-) = K_w \quad \text{(Eq. 4c)}$$

where $K_{a,R}$, $K_{a,HB}$, and K_w are the dissociation constants of drug, buffer, and water, respectively.

Under the assumption of quasi-steady-state conditions existing within the aqueous diffusion layer, the total flux of the drug to the water–lipid interface is expressed by the equation

$$G = -D_{RH}\frac{d(RH^+)}{dx} - D_R\frac{d(R)}{dx} \quad \text{(Eq. 5)}$$

$$(-h \leq x \leq -0)$$

where G is the total flux of the drug and D_{RH} and D_R are the diffusion coefficients; upon integration, the solution is

$$Gh = D_{RH}(RH^+)_{-h} + D_R(R)_{-h} - D_{RH}(RH^+)_{-0} - D_R(R)_{-0} \quad \text{(Eq. 6)}$$

In an analogous procedure for the buffer species,

$$D_{HB}(HB)_{-h} + D_B(B^-)_{-h} - D_{HB}(HB)_{-0} - D_B(B^-)_{-0} = 0 \quad \text{(Eq. 7)}$$